On the transparency of nanostructured alumina: Rayleigh-Gans model for anisotropic spheres.

Carlos Pecharromán,[1]*Gustavo Mata-Osoro,[1] L. Antonio Díaz,[2] R. Torrecillas,[2] J. S. Moya[1]

[1]*Instituto de Ciencia de Materiales de Madrid, (CSIC), C/ Sor Juana Inés de la Cruz, 3, 28049 (Madrid), Spain. cpg@icmm.csic.es*

[2]*Centro de Investigación en Nanomateriales y Nanotecnología (CINN), (CSIC), C/Francisco Pintado Fe, 26, 33011 Oviedo, Spain*

Abstract: A light scattering model under the Rayleigh-Gans-Debye approximation has been developed for polycristalline alumina. The model states that transmittance of dense alumina ceramics basically depends not only on the maximum grain size but also on the preferential orientation of their *c*-axis, or texture. The effect of texture in transparency has been experimentally measured on several dense alumina samples with different grain size and compared to that obtained from x-ray Rietveld refinements with a very good agreement. The Rayleigh-Gans-Debye approximation also allows to represent optical data in a very simple way (logarithm of transmittance vs. the inverse of the wavelength square). Using these variables, a straight line is obtained for the Rayleigh-Gans-Debye approximation, its slope being proportional to the maximum grain size and textural parameter. Deviation from this law implies the presence of pores or grain of extremely large size.

OCIS Codes: (160.1245) Artificially engineered materials; (290.5825) Scattering theory; (260.1440) Birefringence; (350.3850) Materials processing; (160.1190) Anisotropic optical materials.

References and links

1. G. Wei, "Transparent ceramic lamp envelope materials," J. Phys. D **38**, 3057-3065 (2005).
2. U. Anselmi-Tamburini, J. N. Woolman, and Z. A. Munir, "Transparent nanometric cubic and tetragonal zirconia obtained by high-pressure pulsed electric current sintering," Adv. Funct. Mater. **17**, 3267-3273 (2007).
3. R. Apetz and M. P. B. van Bruggen, "Transparent alumina: A light-scattering model," J. Amer. Ceram. Soc. **86**, 480-486 (2003).
4. G. Bernard-Granger, C. Guizard, and A. Addad, "Sintering behavior and optical properties of yttria," J. Amer. Ceram. Soc. **90**, 2698-2702 (2007).
5. R. Fedyk, D. Hreniak, W. Lojkowski, W. Strek, H. Matysiak, E. Grzanka, S. Gierlotka, and P. Mazur, "Method of preparation and structural properties of transparent YAG nanoceramics," Opt. Mater. **29**, 1252-1257 (2007).
6. N. Frage, S. Cohen, S. Meir, S. Kalabukhov, and M. P. Dariel, "Spark plasma sintering (SPS) of transparent magnesium-aluminate spinel," J. of Mater. Sci. **42**, 3273-3275 (2007).
7. A. Krell and J. Klimke, "Effects of the homogeneity of particle coordination on solid-state sintering of transparent alumina," J. Amer. Ceram. Soc. **89**, 1985-1992 (2006).
8. J. G. Li and Y. P. Ye, "Densification and grain growth of Al2O3 nanoceramics during pressureless sintering," J. Amer. Ceram. Soc. **89**, 139-143 (2006).
9. Z. J. Shen, M. Johnsson, Z. Zhao, and M. Nygren, "Spark plasma sintering of alumina," J. Amer. Ceram. Soc. **85**, 1921-1927 (2002).
10. V. V. Srdic, M. Winterer, and H. Hahn, "Sintering behavior of nanocrystalline zirconia prepared by chemical vapor synthesis," J. Amer. Ceram. Soc. **83**, 729-736 (2000).
11. Y. T. O, J. B. Koo, K. J. Hong, J. S. Park, and D. C. Shin, "Effect of grain size on transmittance and mechanical strength of sintered alumina," Mat. Sci. Eng. A **374**, 191-195 (2004).
12. J. Peelen and R. Metselaar, "Light-scattering by pores in polycrystalline materials-transmission properties of alumina" J. Appl. Phys. **45**, 216-220 (1974).

#107558 - $15.00 USD Received 13 Feb 2009; revised 18 Mar 2009; accepted 21 Mar 2009; published 10 Apr 2009

13. T. Kappen, "Status quo of ceramic material for metal halide discharge lamps," J. Phys. D **38**, 3033-3039 (2005).
14. A. Jones, "Light scattering for particle characterization," Prog. Ener, Comb. Sci. **25**, 1-53 (1999).
15. J. Holoubek, "Simple representation of small-angle light-scattering from an anisotropic sphere" J. Polymer Sci. A-2 **10**, 1461 (1972).
16. Y.L. Geng, X.-B. Wu, L. W. Li, and B.R. Guan, "Mie scattering by a uniaxial anisotropic sphere," Phys. Rev. E, **70** 056609 (2004).
17. R. Haracz, L. D. Cohen and A. Cohen, "Scattering of linearly polarized-light from randomly oriented cylinders and spheroids," J. Appl. Phys. **58**, 3322-3327 (1985).
18. L. Turner, "Rayleigh-Gans-Born light-Scattering by ensembles of randomly oriented anisotropic particles," Appl. Opt. **12**, 1085-1090 (1973).
19. G. Bernard-Granger and C. Guizard, "Influence of MgO or TiO_2 doping on the sintering path and on the optical properties of a submicronic alumina material," Scripta Mater. **56**, 983-986 (2007).
20. D. Jiang, D. M. Hulbert, U. Anselmi-Tamburini, T. Ng, D. Land, A. K. Mukherjee, "Optically transparent polycrystalline Al_2O_3 produced by spark plasma sintering" J. Amer. Ceram. Soc. **91**, 151-154 (2008).
21. G. Bernard-Granger, C. Guizard, and A. Addad, "Influence of co-doping on the sintering path and on the optical properties of a submicronic alumina material," J. Amer. Ceram. Soc. **91**, 1703-1706 (2008).
22. D. Chakravarty, S. Bysakh, K. Muraleedharan, T.N. Rao, R. Sundaresan, "Spark plasma sintering of magnesia-doped alumina with high hardness and fracture toughness," J. Amer. Ceram. Soc. **91**, 203-208 (2008).
23. H. C. H. C. v. d. Hulst, *Light scattering by small particles*.
24. W. Dollase, "Correction of intensities for preferred orientation in powder diffractometry-application of the March model," J. Appl. Crystal. **19**, 267-272 (1986).
25. E. Guilmeau, D. Chateigner, T. S. Suzuki, Y. Sakka, C. Henrist, and B. Ouladdiaf, "Rietveld Texture Analysis of Alumina Ceramics by Neutron Diffraction," Chem. Mater. **17**, 102-106 (2005).
26. P. P. Beckmann and A. Spizzichino, *The scattering of electromagnetic waves from rough surfaces*. Ed. Artech House Radar Library, Norwood, MA, USA, (1987)
27. C. Pecharroman, F. Gracía, J. P. Holgado, M. Ocaña, A.R. González-Elipe, J. Bassas, J. Santiso, A. Figueras "Determination of texture by infrared spectroscopy in titanium oxide-anatase thin films," J. Appl. Phys. **93**, 4634-4645 (2003).
28. M. Ocaña, C. Pecharromán, F. Gracía, J. P. Holgado, and A. R. González-Elipe. "Analysis of texture and microstructure of anatase thin films by Fourier transform infrared spectroscopy," Thin Solid Films **515**, 1585-1591 (2006).
29. W. Swiatnicki, S. Lartigue-Korinek, and J. Y. Laval"Grain-Boundary structure and intergranular segregation in Al_2O_3," Acta Metal. Mater.**43**, 795-805 (1995).
30. A. Kebbede, J. Parai, and A. H. Carim, "Anisotropic grain growth in alpha-Al_2O_3 with SiO_2 and TiO_2 additions," J. Amer. Ceram. Soc. **83**, 2845-2851 (2000).
31. Y. Sakka, T.S. Suzuki, and T. Uchikoshi "Fabrication and some properties of textured alumina-related compounds by colloidal processing in high-magnetic field and sintering," J. Eur. Ceram. Soc. **28**, 935-942 (2008).

1. Introduction

The development of new optoelectronic devices has extended the use of ordinary optical materials to new applications and environments such as temperature (IR) sensor, optical fibre communications, laser interferometers, etc. A considerable fraction of these new devices operates inside aggressive environments, such as ovens, radiation chambers and aerospace sensors. In such cases, the sensitive electronic component must be preserved from the extreme external condition by a transparent window. However, most of ordinary optical transparent materials, glasses, polymers, alkali hydrides, or single crystal are expensive, soft, weak and/or brittle. Nowadays the only suitable materials suitable for extreme conditions are only some transparent oxide single crystals *[1]*, as corundum, spinel, yttria and YAG. However the growing and machining of single crystals is an expensive task, which largely limit the scale up of production of those materials.

In this sense, several groups [2-11] have developed transparent and translucent ceramics with different optical and mechanical properties. However, the light scattering due to the presence of small pores has been found to be the main problem to overcome in this particular kind of materials [12]. In order to minimize, and even to fully eliminate any pore light scattering, the remaining porosity must be smaller than its experimental detection error (0.5%) and additionally, the pore size should be kept as small as possible. The Rayleigh criterion

#107558 - $15.00 USD Received 13 Feb 2009; revised 18 Mar 2009; accepted 21 Mar 2009; published 10 Apr 2009

determines that it should be at least 10 times smaller than the incident wavelength, which, in the case of optical radiation, means that the maximum pore size must be smaller than 10 nm. Considering that pore size is closely related with the average ceramic grain size [10], nanostructured ceramics are the optimal candidate to fabricate transparent ceramics.

From all the materials employed to sinter transparent ceramics, the alumina is the one with the best mechanical properties, such as hardness, flexure strength and chemical stability. In fact, Lucalox® alumina is the only commercial material used nowadays for high power lightening[13]. Depending on the sintering treatment, several light scattering processes need to be considered to understand the optical response of dense alumina ceramics, i.e., the pore and grain scattering. The measurement of transmittance for a large range of wavelength will allow to determine the nature of light scattering. In fact, for pore and small grain size scattering (compared to the incident wavelength), the absorbance coefficient is given by the Rayleigh scattering regime so that it is proportional to $(a/\lambda)^4$ (where a stands for the scatter radius and λ the incident wavelength). In the particular case where the grain size is comparable to the wavelength, the scattering follows a $(a/\lambda)^2$ law known as Rayleigh-Gans-Debye or RGD. Finally, if the wavelength is much shorter than the grain size, the scattering becomes wavelength independent as it corresponds to the anomalous diffraction regime (AD). In this sense it is crucial to determine the nature and the efficiency of each type of scattering. In particular, Rayleigh scattering by pores should be suppressed because it whiten the samples, spoiling their transparency.

Apart from the pore scattering, the grain scattering exclusively appear in ceramics from anisotropic phases, is due to the small differences in refractive indices at the interfaces of anisotropic crystallites. For α-Al_2O_3 the degree of birefringence, i.e. the difference from the ordinary to the extraordinary refractive indices is small, Δn =0.008 or $\Delta n/n=4.5\cdot10^{-3}$ (n_o = 1.7638 and n_e = 1.7556 at 700 nm) but enough to whitens most of alumina ceramics.

Although the problem of light scattering by anisotropic particles has been treated by several authors applied to liquid crystals, meteorology, etc [14-18] the standard model presently used to describe the transparency of alumina ceramics was introduced by Apetz et al[3]. This model is basically a phenomenological modification of the RGD originally developed for isotropic spheres. The most relevant result is the λ^{-2} law of the absorbance for forward scattering, which also depends linearly on the crystallite size and on an anisotropy parameter. This model satisfactorily reproduces the optical transmittance of some near-free porosity alumina samples presented in the literature [3,7-9,19,20]. However, the physical meaning of the effective birefringence, which in this model is a fitting parameter, is unclear. In this sense, it is hard to determine which are the optimal conditions to reduce grain scattering. Indeed, it is even possible to find in the literature samples exhibiting similar average grain size but different optical response [3,8,11,19-22].

In the present work we introduce a rigorous deduction of the absorbance for a set of anisotropic particles in the RGD regime. In order to describe the microstructure of a set of uniaxial crystallites, apart from the grain size distribution, some texture information is also required. This model will allow to better understand the process of light scattering in dense anisotropic ceramics as well as become an appropriate tool to design nanostructured transparent alumina materials.

2.Theoretical background

The phenomena related with light scattering by particles can be fully described by the solution of the Mie equation. However, the use of this method is cumbersome due to the large amount of calculation resources it requires. Instead, several approximation have been developed to obtain simple analytic expressions for describing the scattering processes. In this sense, the light scattering by anisotropic grains of alumina ,with a size not much larger than the incident wavelength, can be treated as a “low contrast” approach. In this case, the scatter centres are the crystallites that present a slight difference of refractive index to the light beam propagating

#107558 - $15.00 USD Received 13 Feb 2009; revised 18 Mar 2009; accepted 21 Mar 2009; published 10 Apr 2009

along the ceramic. In this context, we have chosen the Rayleigh-Gans-Debye (RGD) approximation, which is valid for small scatters with a refractive index very similar to that of the environment ($|m-1|<<1$ and $2\pi|m-1|a/\lambda<<1$, where m is the quotient between the refractive index of the scatter and that of the surrounding medium. This model has been well established for isotropic materials[23]. For the present case, i.e. alumina transparent ceramics, the model must be rederived assuming that the polarizability of each scatter element is now a tensor instead of a constant. For a sake of simplicity, we consider that the whole system has an average refractive index, n_{av} which is very similar to those of the single crystal, n_o and n_e..

The light intensity can be easily calculated as:

$$I_s(\theta,\zeta,\phi) = \left|E_{s\perp}\right|^2 + \left|E_{s\parallel}\right|^2 \tag{1}$$

where ξ and ϕ are the angle of the optical axis of a singular crystallite with the sample surface normal and the incidence plane respectively (Fig. 1).

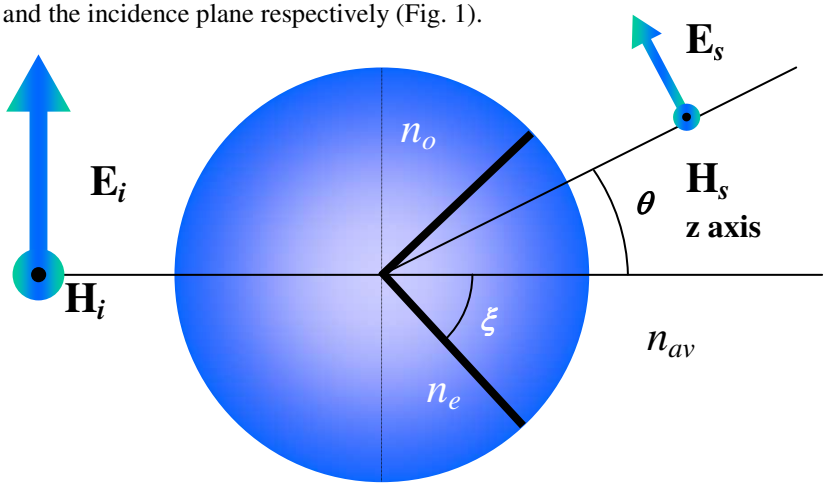

Fig.1. Geometry of the incident field (**E***i*, **H***i*), anisotropic sphere, with refractive index n_e and n_o and scattered beam (**E***s*, **H***s*).

We suppose that the ceramic has an azimuth symmetry (samples have a flat shape and the symmetry axis is perpendicular to the largest surface) so that, the intensity is given by the angular average with respect to ϕ.

$$I(\theta,\zeta) = \frac{1}{2\pi}\int_{-\pi}^{\pi} I(\theta,\xi,\phi)d\phi \tag{2}$$

The scattered intensity is given by:

$$I = \frac{\int_0^{2\pi}\left|\vec{E}_{s\parallel}\right|^2 + \left|\vec{E}_{s\perp}\right|^2 d\phi}{2\pi} \tag{3}$$

In this sense, it is necessary to determine the scattered field. The contribution of each volume differential to the far scattered field is given by the electric field induced by the corresponding dipolar moment:

$$dE_j = \frac{k^2}{4\pi\in_0 \varepsilon_{av} r} e^{-ikr}\left(\vec{u}_r \times d\vec{p} \times \vec{u}_r\right) \tag{4}$$

Where $\boldsymbol{\varepsilon}_{av}$ is the effective dielectric constant outside the scatter and $\in_0$ the vacuum permittivity. After some manipulations it results:

#107558 - $15.00 USD Received 13 Feb 2009; revised 18 Mar 2009; accepted 21 Mar 2009; published 10 Apr 2009

$$dE_{s\|} = \frac{k^2}{4\pi \in_0 \varepsilon_{av} r} e^{-ikr} \left(dp_x \cos\theta - dp_z \sin\theta \right)$$
$$dE_{s\perp} = \frac{k^2}{4\pi \in_0 \varepsilon_{av} r} e^{-ikr} dp_y \tag{5}$$

In the case of anisotropic crystals, the total dipolar moment induced by a single particle is given by

$$\vec{p} = \int_{V'} \tilde{\alpha}(\vec{r}\,') \vec{E}(\vec{r}\,')\, dV' \tag{6}$$

where α is the polarizability tensor. In the case of the small contrast approximation, i.e. ε_o and ε_e the main values of the dielectric tensor $\boldsymbol{\varepsilon}_r$ are very close to $\boldsymbol{\varepsilon}_{av}$, the incident electric field is assumed to be constant and the polarizability of a particle with arbitrary shape can be approximated as:

$$d\tilde{\boldsymbol{\alpha}} = \in_0 \left(\tilde{\boldsymbol{\varepsilon}}_r - \tilde{\boldsymbol{\varepsilon}}_{av} \right) dV' \tag{7}$$

The dielectric expression of dielectric tensor for any possible orientation is given by:

$$\tilde{\varepsilon}_r - \tilde{\varepsilon}_{av} = \mathbf{P} \begin{pmatrix} \varepsilon_o - \varepsilon_{av} & 0 & 0 \\ 0 & \varepsilon_o - \varepsilon_{av} & 0 \\ 0 & 0 & \varepsilon_e - \varepsilon_{av} \end{pmatrix} \mathbf{P}^{-1} \tag{8}$$

where the **P** matrix accounts for the change of base referring to the principal axes of the dielectric tensor of the particle. We define the angle ξ as the angle of the third component of the dielectric tensor with the incident wavevector. In order to simplify the notation, we introduce the following parameters, r_o, r_e and Δ, defined as follows:

$$\begin{cases} \varepsilon_o = \varepsilon_{av} - r_o \Delta \\ \varepsilon_e = \varepsilon_{av} + r_e \Delta \end{cases} \tag{9}$$

$$\begin{cases} r_o + r_e = 1 \\ \varepsilon_e - \varepsilon_o = \Delta \end{cases} \tag{10}$$

Operating Eq. (6) results:

$$d\vec{p} = \frac{\in_0 \Delta}{\sqrt{2}} \begin{pmatrix} -r_o + \frac{1}{2}\sin^2\xi \left(1 + \cos 2\phi + \sin 2\phi\right) \\ -r_o + \sin^2\xi \sin\phi \left(\cos\phi + \sin\phi\right) \\ \cos\xi \sin\xi \left(\cos\phi + \sin\phi\right) \end{pmatrix} dV \tag{11}$$

and Eq. (5) becomes:

$$dE_{s\|} = \frac{k^2}{4\pi\varepsilon_{av} r} e^{-ikr} \frac{\Delta}{\sqrt{2}} \begin{Bmatrix} \cos\theta \left[-r_o + \frac{1}{2}\sin^2\xi \left(1 + \cos 2\phi + \sin 2\phi\right) \right] \\ -\sin\theta \left[\cos\xi \sin\xi \left(\cos\phi + \sin\phi\right) \right] \end{Bmatrix} dV$$
$$dE_{s\perp} = \frac{k^2}{4\pi\varepsilon_{av} r} e^{-ikr} \frac{\Delta}{\sqrt{2}} \left[-r_o + \sin^2\xi \sin\phi \left(\cos\phi + \sin\phi\right) \right] dV \tag{12}$$

According to the Rayleigh-Gans approximation, the scattered field is calculated by integrating each volume element independently of the other volume elements. As a result, only a phase factor $e^{i\delta}$ must be considered for integration to result the function $R(\theta)$[23]. In the case of anisotropic spheres, the $R(\theta)$ function is not identical to that of the spherical ones, but it can be showed that the difference is just an infinitesimal of Δ, and can be neglected. As a result, the light intensity (eq. (3)) is given by:

#107558 - $15.00 USD Received 13 Feb 2009; revised 18 Mar 2009; accepted 21 Mar 2009; published 10 Apr 2009

$$I = I_0 \frac{k^4 V^2 \left|R(\theta)\right|^2}{\left(4\pi r \varepsilon_{av}\right)^2} \Delta^2 \left[\frac{\left(1+\cos^2\theta\right)}{2} \cdot \frac{3-8\,r_o+16\,r_o^2+\left(8\,r_o-4\right)\cos 2\xi+\cos 4\xi}{16} + \frac{\sin^2\theta \sin^2 2\xi}{8} \right] \quad (13)$$

This expression has two components. The first one is identical to that of isotropic spheres which depends on $(1+\cos^2\theta)$ but multiplied by a polynomial in $\cos\xi$. For the present system, an additional new term appears, which depends on $\sin^2\theta$, coming from the non-zero contribution of p_z. In order to calculate the scattering cross section, a integral around θ must be done. The result is:

$$Q_{sca} = \frac{\Delta n^2}{n_{av}^2}\left[\Phi_1(x)\alpha(\xi, r_o) + \Phi_2(x)\beta(\xi, r_o)\right] \quad (14)$$

Where $x = k \cdot a$ being k the wavevector and a the crystallite radius. The coefficients α and β, which depend on the crystallite orientation, ξ,, are given by:

$$\alpha(\xi, r_o) = \frac{3-8\,r_o+16\,r_o^2+\left(8\,r_o-4\right)\cos 2\xi+\cos 4\xi}{4}$$
$$\beta(\xi, r_o) = \sin^2 2\xi \quad (15)$$

In order to determine the relationship from the variables r_o and r_e to the textural information, given by ξ, it is necessary to determine the effective value of the dielectric constant ε_{av}. For such purpose, an effective medium model developed for dense anisotropic materials formed by equiaxial crystallites and have been applied[27].

$$\left(1+c_{pez}\right)\frac{\left(\varepsilon_{av}-\varepsilon_o\right)}{(1-L)\varepsilon_{av}+\varepsilon_o} + \left(1-c_{pez}\right)\frac{\left(\varepsilon_{av}-\varepsilon_e\right)}{2L\varepsilon_{av}+(1-2L)\varepsilon_e} = 0 \quad (16)$$

The Eq. (16) can be simplified if ε_o and ε_e are very close (low contrast approximation), and taking into account the definition of r_o and r_e (eq. (9))we get:

$$r_o = \frac{1-c_{pez}}{2}$$
$$r_e = \frac{1+c_{pez}}{2} \quad (17)$$

where c_{pez} is the term which carries on the textural information of the ceramic. This term, according to reference [27] is defined as follows:

$$c_{pez} = 1/4\pi \int \cos^2(\psi)\Gamma_{pe}(\psi)\,d\Omega \quad (18)$$

where $d\Omega$ is the solid angle differential and Γ_{pe} the probability density function corresponding to the angular orientation of the extraordinary optical axis. A estimation of coefficient c_{pex} was described in reference [27] as a function of ξ.

$$c_{pez}(\xi) = \frac{\cos^2(\xi)}{1+\sin^2(\xi)} \quad (19)$$

Combining Eq.s (17) with (19) results:

$$r_o = \frac{\sin^2\xi}{1+\sin^2\xi}$$
$$r_e = \frac{1}{1+\sin^2\xi} \quad (20)$$

Finally the functions (15) $\alpha(\xi)$ and $\beta(\xi)$can be written as:

#107558 - $15.00 USD Received 13 Feb 2009; revised 18 Mar 2009; accepted 21 Mar 2009; published 10 Apr 2009

$$\alpha(\xi)=\frac{\left(11-4\cos(2\xi)+\cos(4\xi)\right)\sin^4(\xi)}{\left(\cos(2\xi)-3\right)^2} \tag{21}$$

$$\beta(\xi)=\sin^2 2\xi \tag{22}$$

The angular dependence of the $\alpha(\xi)$ function appear in Table I and Fig. 2.

Table I. Values of $\alpha(\xi)$ calculated versus the orientation angle, calculated each 5º

ξ	$\alpha(\xi)$	ξ	$\alpha(\xi)$
0	0	50	0.36771
5	0.00011368	55	0.46771
10	0.0017151	60	0.57398
15	0.0079185	65	0.68118
20	0.022236	70	0.78274
25	0.047394	75	0.87156
30	0.085	80	0.94082
35	0.13583	85	0.98488
40	0.20015	90	1
45	0.27778		

On the other hand, the functions $\Phi_1(x)$ and $\Phi_2(x)$ are given by:

$$\Phi_1(x)=\frac{5}{2}+2x^2-\frac{7\left(1-\cos 4x\right)}{16x^2}-\frac{\sin 4x}{4x}-\left(2-\frac{1}{2x^2}\right)\left(\gamma-\mathrm{Ci}(4x)+\ln 4x\right) \tag{23}$$

$$\Phi_2(x)=3\left(\frac{1-\cos 4x}{8x^2}-1\right)+\frac{\sin 4x}{2x}+\left(2-\frac{1}{2x^2}\right)\left(\gamma-\mathrm{Ci}(4x)+\ln 4x\right) \tag{24}$$

Because it is not straightforward to evaluated the functions $\Phi_1(x)$ and $\Phi_2(x)$, it is more convenient to use their asymptotic expansions when $x\to 0$ and $x\to\infty$.

$$\Phi_1(x)\simeq\begin{cases}\frac{32}{27}x^4 & \text{if} \quad x\to 0\\ 2x^2 & \text{if} \quad x\to\infty\end{cases} \quad (25)\quad \Phi_2(x)\simeq\begin{cases}\frac{16}{27}x^4 & \text{if} \quad x\to 0\\ -3+2\gamma+\ln 16+2\ln x & \text{if} \quad x\to\infty\end{cases} \tag{26}$$

In both cases, $\Phi_1(x)$ and $\Phi_2(x)$, exhibit a x^4 power law dependence for longer wavelengths corresponding to the Rayleigh scattering. In the case of short wavelength, $\Phi_1(x) >> \Phi_2(x)$ so that $\Phi_2(x)$ can be neglected. As a result, the approximations (25) and (26) into Eq. (1.1) can be written as follows:

$$Q(x,\xi)=\begin{cases}2x^2\frac{\Delta n^2}{n_{av}^2}\frac{\left(11-4\cos(2\xi)+\cos(4\xi)\right)\sin^4(\xi)}{\left(\cos(2\xi)-3\right)^2} & \text{if} \quad x\gg 1\\ \frac{32}{27}x^4\frac{\Delta n^2}{n_{av}^2}\frac{\left(13-4\cos(2\xi)-\cos(4\xi)\right)\sin^2(\xi)}{\left(\cos(2\xi)-3\right)^2} & \text{if} \quad x\ll 1\end{cases} \tag{27}$$

The two components of expression (27) corresponds to the RGD and the Rayleigh approximations respectively. In case of nanostructured alumina ceramics, an according to expression (27), the crossover from scattering corresponding to the Rayleigh and RGD

#107558 - $15.00 USD Received 13 Feb 2009; revised 18 Mar 2009; accepted 21 Mar 2009; published 10 Apr 2009

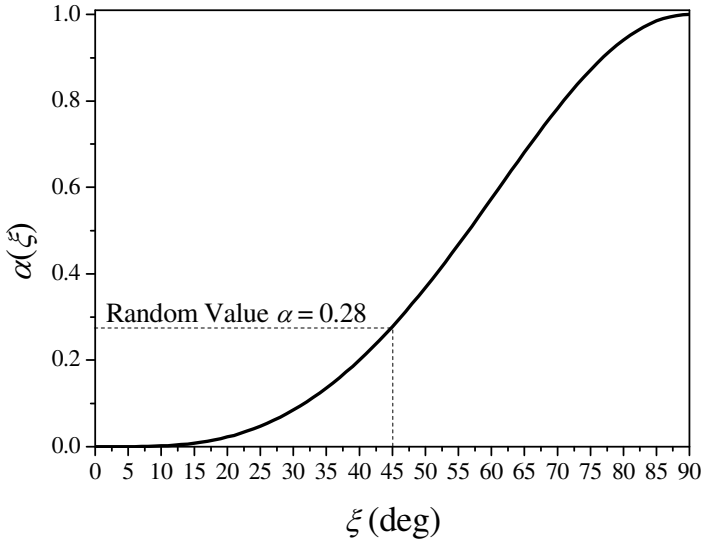

Fig. 2. Textural function $\alpha(\xi)$ that appear in the RGD scattering approximation vs. the preferential textural angle ξ.

regimes appears at wavelengths close to 1000 nm. For longer wavelengths, the scattering losses are considerably smaller than those due to the surface reflectance (which are about of 14%) so that we are going to focused on the short wavelength region and therefore on the RGD approximation. In this sense, the efficiency scattering can be rewritten as:

$$Q(x,\xi) = 2x^2 \frac{\Delta n^2}{n_{av}^2} \alpha(\xi) \tag{28}$$

being $\alpha(\xi)$ the texture function given by Eq. (21).

The transmittance of a thick ceramic layer (neglecting interference effects) is given by

$$R.I.T. = \left[1 - 2\left(\frac{n_{av}-1}{n_{av}+1}\right)^2\right] e^{-\kappa d} \tag{29}$$

$$\kappa = \pi a^2 Q_{sca} N = f \frac{3}{4} \frac{Q_{sca}}{a} \tag{30}$$

where κ is the absorbance coefficient, d the ceramic thickness, N the number of crystallites per volume and f the scatter volume concentration. In the case of a dense ceramic formed by crystallites with identical size, f = 1. However, in the case of an heterogeneous grain size distribution, Eq. (30) must be written as:

$$\kappa = \sum_i f_i \, a_i \frac{6\pi^2}{\lambda^2} \Delta n^2 \alpha(\xi) \tag{31}$$

where the value of the partial concentration of spheres of radius a_i is given by:

$$f_i = \frac{a_i^3}{\sum_i a_i^3} \tag{32}$$

#107558 - $15.00 USD Received 13 Feb 2009; revised 18 Mar 2009; accepted 21 Mar 2009; published 10 Apr 2009

Accordingly, the absorbance coefficient for uniaxial grain scattering is given by:

$$\kappa = \left\langle a_g \right\rangle \frac{6\pi^2}{\lambda^2} \Delta n^2 \alpha(\xi) \tag{33}$$

where $\langle a_g \rangle$ is the medium value corresponding to the volume grain distribution, defined by:

$$\left\langle a_g \right\rangle = \sum_i a_i f_i = \frac{\sum_i a_i^4}{\sum_i a_i^3} \tag{34}$$

This can be considered a very relevant result because Eq. (34) clearly states that for heterogeneous grain size distribution, $\langle a_g \rangle$ can be estimated, with a good degree of approximation, be similar to the maximum value of experimentally found grain radius.
Finally Eq. (29) can be written as:

$$\log\left(R.I.T.\right) = \log\left(T_0\right) - \frac{6\pi^2 \left\langle a_g \right\rangle}{\lambda^2} \Delta n^2 \alpha(\xi) d \tag{35}$$

Thus, a quadratic fit of log(*R.I.T.*) vs. λ^{-2}, will produce a line. The slope of the line is proportional to the values of $\alpha(\xi)$ and because the rest of magnitudes present in Eq. (35) can be experimentally measured, the texture parameter can be estimated by this simple way. Finally, the crossing of this line with the ordinates axis must correspond to the logarithm of the transmittance of a scattering free sample.

3. Experimental

High purity α-Alumina (99.99%) (TM-DAR, Taimei Chemicals Co., LTD.), with an average particle size of d_{50}=0.2 μm, a BET specific surface area of 14.5 m^2/g and the following chemical analysis (ppm): Si (10), Fe (8), Na (8), K (3), Ca (3), Mg (2), Cu (1), Cr (<1), Mn (<1), U (<0.004), Th (<0.005) has been used as starting powder.

Powder suspensions of 60 wt% solid content were prepared using distilled water as liquid media and a 0.5 wt% addition of an alkali-free organic polyelectrolyte as surfactant (Dolapix DE-64). The pH of the obtained suspension was found to be 8.8±0.1 .The suspensions were homogenised by milling with alumina balls, 99.9% purity, in polyethylene containers at 150 r.p.m. for 24 h. After homogenized, the mixtures were de-aired while stirring for one hour . The slip casting process to obtain green plates (10×10×1 mm) was performed in an alumina mould and under vacuum in order to eliminate bubbles.

The samples were sintered in an electrical controlled (±1ºC) tubular alumina (99.7% purity) furnace. This furnace has an attached vacuum system which allows to sinter to 1600ºC at 10^{-6} mbars. All the cast green plates were burn out at 800ºC for 24h in air atmosphere to avoid the presence of organic residues. Afterwards, the samples were sintered up to 98% th. densities at 1350º, 1400º, 1450º , 1500º and 1600º C. Finally the samples sintered at 1400º and 1500º C for 2h were Hot Isostatic Pressed (HIP), at 1100º C and 1000 bar for 1 hour.

The microstructure of fired plates was studied after a thermal etching (for 1h at temperature 15% lower than that used during sintering) on polished surfaces down to 1 μm by Scanning Electron Microscopy (SEM, Hitachi, model S3000N) and AFM (Nanotec) with 2nm curvature radius probes (Nanosensors).

The sintered plates were polished on both sides to eliminate surface scattering. The transmittance spectra were measured using three spectrophotometers: a Nicolet 20 SXC Fourier transform infrared FTIR spectrophotometer were used from 5 to 2.5 μm, a Bruker IFS 66V from 2.5 to 0.8um, and finally a Varian Cary 4000 for the visible range (0.8 to 0.3μm).

#107558 - $15.00 USD Received 13 Feb 2009; revised 18 Mar 2009; accepted 21 Mar 2009; published 10 Apr 2009

X-ray diffraction measurements were taken in a Bruker D8 for texture determination by Rietveld refinements [24].

4. Results

The visible to IR spectra of the different studied samples appears in Fig. 3(a). Fig. 3(b) corresponds to a picture of pieces of the four studied samples.

Two of these samples have been pressureless sintered at high vacuum (1350ºC and

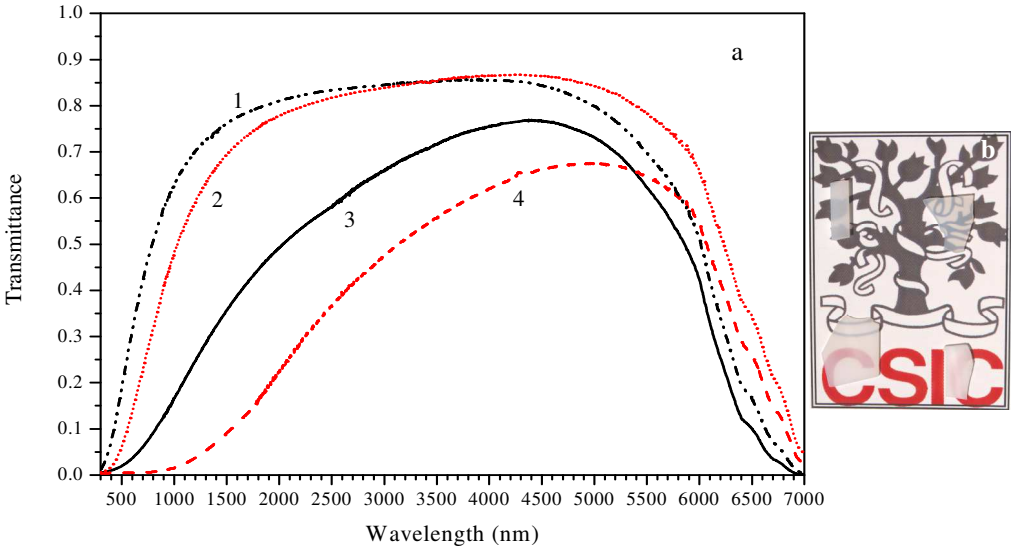

Fig. 3. (a) Experimental optical transmittance vs. wavelength for the four considered samples: 1) sintered at 1400º C for 2h at vacuum followed by HIP; 2) sintered at 1500º C for 2h at vacuum followed by HIP; 3) sintered at 1350º C for 50h at vacuum; 4) sintered at 1600º C for 50h at vacuum. (b) External aspect of the four samples.

1600ºC) for a period of 50h. The other two samples were also pressureless sintered at high vacuum at 1400 and 1500ºC for just 2 hours to then be hot isostatic pressed . The transmittance of these two later samples is remarkable good, specially in the visible spectral region. According to expression (35), curves corresponding to Fig. 3(a) have been reploted transformed as log (T) vs. $1/\lambda^2$ in Fig. 4.

In Fig. 4 the absorbance spectra vs. λ^{-2} of the selected samples appear. According to Eq. (35) a linear fit is expected. In general, the spectra fit quite well. However, pressureless sintered samples (1350º and 1600ºC for 50h) considerably deviate from linear fitting for large values of λ^{-2}. In this sense, we only have considered the lower spectral ranges, where the linearity is satisfied, because for shorter wavelengths, the anomalous diffraction[14, 23] regime saturates the absorbance. The experimentally measured values of thickness,maximum grain size, the Rietveld texture parameter, and the results of fitting, i.e. the texture angle ξ, appear in table II.

#107558 - $15.00 USD Received 13 Feb 2009; revised 18 Mar 2009; accepted 21 Mar 2009; published 10 Apr 2009

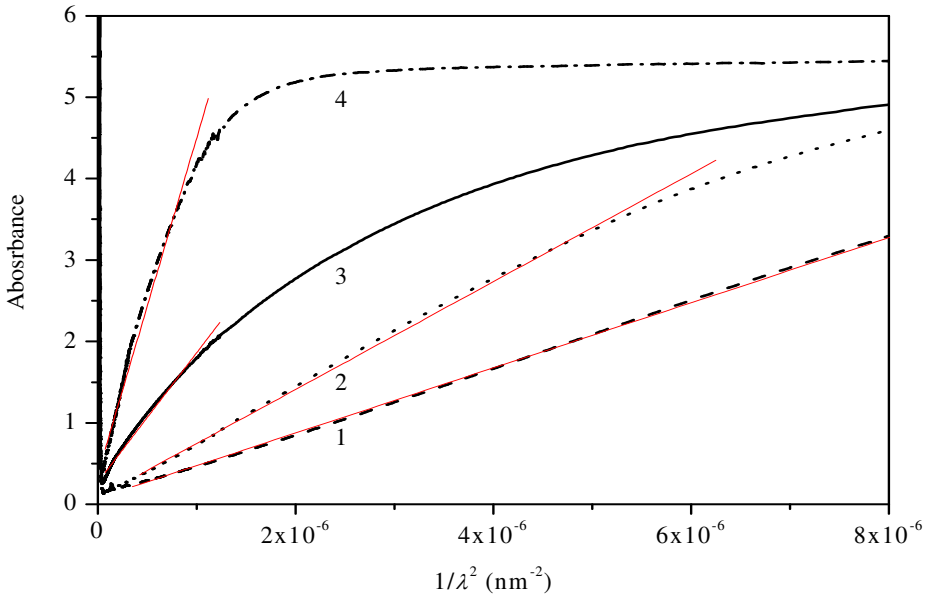

Fig 4. same graphic as figure 3 but representing logarithm of transmittance (absorbance) vs. the inverse of the wavelength square. Straight lines represent the linear fitting in the low wavelength region.

Table II.

	$2\cdot\langle a_g\rangle$ (nm)	d(mm)	$R_{0,\mathrm{fit}}$	α	ξ (deg)	Text. Param.
vac 1350º	1820	1.31	0.71747	0.33748	48.388	0.944
HIP 1400º	1027	1.00	0.89657	0.20074	40.042	0.9
HIP 1500º	2764	0.59	0.92633	0.21666	41.138	0.92
vac 1600º	30000	0.75	0.79836	0.14171	35.505	0.767

Maximum grain size were determined from statistic analysis of AFM and SEM micrographs as it appears in Fig. 5.

#107558 - $15.00 USD Received 13 Feb 2009; revised 18 Mar 2009; accepted 21 Mar 2009; published 10 Apr 2009

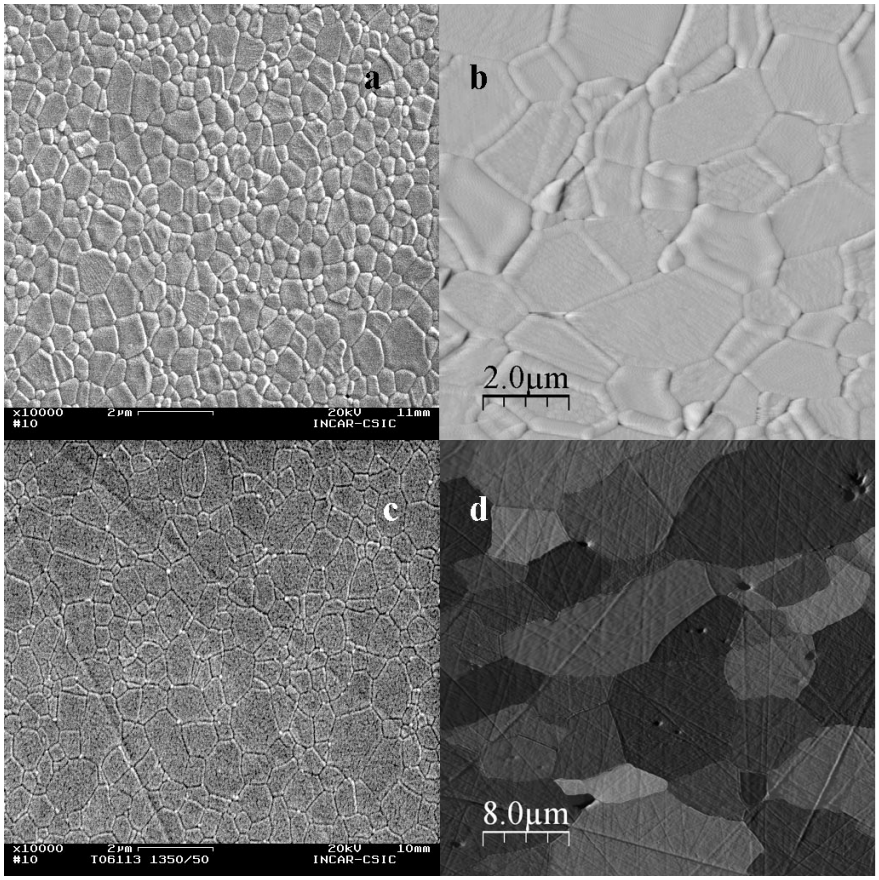

Fig. 5. Microstructure of the four considered samples after a thermal etching. a) SEM image of sample sintered at 1400º C for 2h at vacuum to then HIP; b) SEM image of sample sintered at 1500º C for 2h at vacuum to then HIP; c) AFM image of sample sintered at 1350º C for 50h at vacuum; d) AFM image of sample sintered at 1600º C for 50h at vacuum (the contrast has been enhanced for a better visualization of grains).

X-ray Rietveld analysis have been performed on the four samples. The textural parameters [24, 25] appear in table II. These parameters take a value of 1 for random distribution of crystallites and 0 for textured samples with the (001) planes parallel to the surface slab. Additionally, grain size seems to be somehow related to texture as it appears in Fig. 6 (a).According to the table II, and Fig. 6(b), a clear correlation from optical and diffraction measurements on texture can be observed.

#107558 - $15.00 USD Received 13 Feb 2009; revised 18 Mar 2009; accepted 21 Mar 2009; published 10 Apr 2009

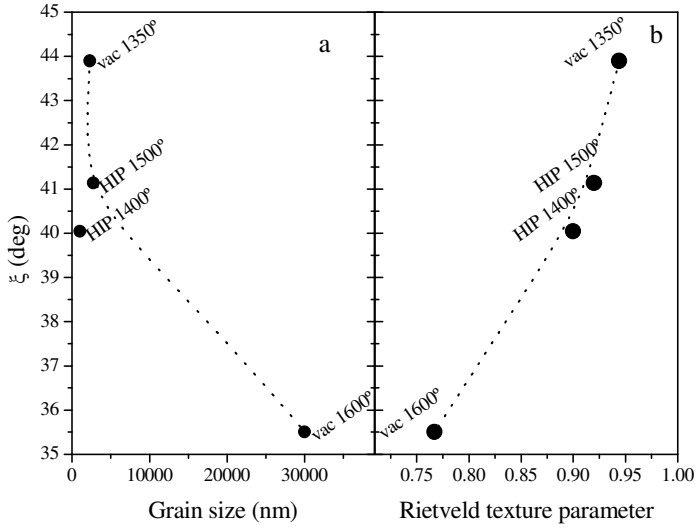

Fig 6. (a) Maximum grain radius $\langle a_g \rangle$ vs. the preferential crystallite angle, ξ, for the considered samples. The continuous line is guide for the eye. (b) Comparison vs. the preferential crystallite angle ξ determined by optical measurements and the x-ray Rietveld texture parameter. The continuous line is guide for the eye.

5. Discussion

The complete understanding of the optical behaviour of transparent and translucent aluminas has been revealed to be a difficult task. Different sources of light scattering may overlap in the same spectral range. We have identified in the alumina ceramics prepared at our laboratory up to five different scattering regimes, i) Rayleigh regime due to pores, ii)surface roughness [26], iii) Rayleigh, iv) RGD and v) anomalous diffraction regimes due to grains. The correct identification of each source of scattering is crucial to determine the quality of the material. Moreover, the analysis of scattering processes is a valuable tool to obtain relevant microstructural information from the samples. For instance, an absorbance dependence following a λ^{-4} law at visible range is a clear indication of residual porosity. The sensitiveness of the optical observations is much larger than that of the standard (Archimedes) method to measure densities. Identically, the saturation of absorbance at shorter wavelengths (Fig. 4) is an evidence of anomalous diffraction regime [14, 23], produced by some proportion of very large crystallites.

However in the case of fully dense transparent alumina samples, RGD scattering due to grains has revealed to be the most relevant one. In this work, it has been stated that this type of scattering and therefore the transparency at infrared and optical wavelengths, depends on the grain size of the largest grains and on their orientation.

In fact, the Apetz et al[3] previous model introduced a phenomenological parameter, Δn_{Apetz}, related to the birefringence constant, $\Delta n = n_e - n_o$. According to Eq. (35), the relationship from Δn_{Apetz} to ξ is given by:

$$\Delta n_{Apetz} = \Delta n \sqrt{2\alpha} \tag{36}$$

$$\Delta n_{Apetz} = \Delta n \sqrt{2\left(11 - 4\cos 2\xi + \cos 4\xi\right)} \frac{\sin^2 \xi}{\cos 2\xi - 3} \tag{37}$$

The Apetz paper stated that the random value for Δn_{Apetz} is $2/3 \cdot \Delta n = 0.0053$. Using Eq. (37) it results a value of ξ=41º which is not far from random orientation ξ=45º according to the

#107558 - $15.00 USD Received 13 Feb 2009; revised 18 Mar 2009; accepted 21 Mar 2009; published 10 Apr 2009

model herewith considered[27, 28]. However, this similitude is just a coincidence. In fact, the random value of Δn_{Apetz} should be $1/3 \cdot \Delta n$, according to the expression

$$\langle n \rangle_{random} = \tfrac{2}{3} n_o + \tfrac{1}{3} n_e \tag{38}$$

$$\Delta n_{Apetz,random} = \langle n \rangle_{random} - n_o = \tfrac{1}{3} \Delta n \tag{39}$$

Fortunately, another mistake in the value of the estimated scattered concentration, assigned to f=1/2 instead of the correct value for dense ceramics f=1, compensates this term.

The texture data obtained from the considered samples seems to indicate that, regardless of the grain size, samples did not present preferential orientation unless they were sintered above 1600ºC (Fig. 6(b)). In order to confirm these results, a further XRD Rietveld analysis of the data, gave no appreciable grain orientation except for the sample heated at 1600ºC for 50h. This is in very good agreement with the optical measurements.

These results closely reproduce the Guilmeau et al [25] previous observations . These authors have studied by neutron diffraction the texture of several alumina samples, sintered at different temperatures. Although in this work, the alumina powders were previously oriented by a 10T magnetic field, the authors observed a remarkable increase of the (001) grain orientation only for the sample sintered at 1600ºC.

According to Eq. (35) the maximum grain size $<a_g>$ and the textural $\alpha(\xi)$ function are correlated in the expression of the transmittance. This fact notably complicates the unambiguous observation of the texture influence into the transparency of alumina ceramics in such manner that textural information have been ignored. As a result, medium grain size has been the only parameter to be considered for explaining the transparency of alumina ceramics. In the present investigation we have stated that the grain size is not the only parameter that determine the optical transmittance, but the relative orientation of the grains must be taken into account as well. In fact, a recent paper [21] has determined that CaO and TiO_2 doped alumina presented Δn_{Apetz} values as small as 0.0028 (note that in the original paper, they refer to a fitting grain size much smaller than the observed one). This value corresponds to a textural orientation of ξ=26º. In fact, it is well known, that doping may induces a preferential growth of some alumina surfaces [29, 30]. In this sense, the knowledge of the role of texture into the transmittance of dense ceramic opens new and more efficient ways to increase the transparency of polycrystalline aluminas. Moreover, three different procedures have been shown to be effective to induce a preferential (001) texture, i.e., powder conforming under strong magnetic fields [31], sintering above 1600ºC [25] and doping [21].

The herewith presented theoretical model, in combination with a careful powder processing and an appropriated choice of some of those grain orientation mechanisms, will allow, “a priori”, to design the critical fabrication parameters to achieve transparency in polycrystalline aluminas.

6. Conclusions

A theoretical model for light scattering for polycrystalline aggregates of uniaxial spheres has been proposed on the basis of the Rayleigh-Gans-Debye approximation. This model shows that each individual grain, which is considered to be a single crystal, scatters light, and the scattering efficiency depends linearly on the grain size and on the relative orientation of grains (texture) through a parameter called $\alpha(\xi)$. Additionally, it presents the characteristic λ^{-2} dependence corresponding to a RGD light scattering process. Several transparent and translucent alumina samples have been analysed showing all of them a spectral region in which the RGD scattering is present. From a simple linear fitting of the optical absorbance versus λ^{-2} it has been possible to determine a textural parameter, that agrees very satisfactorily to the one obtained from x-ray Rietveld analysis. On the base of the proposed scattering model, it is now possible to design the most reliable fabrication route to obtain transparent aluminas.

#107558 - $15.00 USD Received 13 Feb 2009; revised 18 Mar 2009; accepted 21 Mar 2009; published 10 Apr 2009